American Mineralogist, Volume 89, pages 807–811, 2004

The flux growth of magnesium silicate perovskite single crystals

DAVID P. DOBSON[1,*] AND STEVEN D. JACOBSEN[2,†]

[1]Department of Earth Sciences, University College London, Gower Street, London, WC1E 6BT, U.K.
[2]Bayerisches Geoinstitut, Universität Bayreuth, D-94550 Bayreuth, Germany

ABSTRACT

We present a flux-growth method for growing large, strain- and inclusion-free single crystals of perovskite-type $(Mg,Fe,Al)(Si,Al)O_3$ in a multi-anvil apparatus. Molten NaCl is used as the flux and the temperature is cycled at ~25 GPa to enhance grain growth. In this way, we have synthesized high-quality subhedral perovskite crystals in excess of 300 micrometers of pure Mg, or Fe- and Al-bearing compositions with minimal Na-contamination from the flux. Single-crystal structure refinement of the $MgSiO_3$-perovskite demonstrates the quality of the crystals.

INTRODUCTION

Magnesium silicate perovskite ($MgSiO_3$) (hereafter Mg-perovskite) is thought to be the major phase in the Earth's lower mantle (660–2900 km depth), making it the most abundant silicate in the planet. Comparisons between the experimentally determined physical properties of Mg-perovskite (in particular, *P-V-T* equations of state, sound velocities, and electrical conductivity) and geophysically based Earth models such as PREM (Dziewonski and Anderson 1981) therefore yield important information on the physical and chemical state of the Earth's lower mantle. The Mg-perovskite phase in Earth's lower mantle is also likely to contain various amounts of minor chemical components, which can significantly affect its physical properties (Xu et al. 1998; Xu and McCammon 2002; Xhang and Weidner 1999; Brodholt 2000). In particular, heterovalent substitutions can significantly affect the transport and elastic properties of Mg-perovskite through the introduction of electronic and vacancy defects. Ferric iron on the cation site, for example, greatly enhances the electrical conductivity of perovskite (Xu et al. 1998). The most highly studied heterovalent subsitiutions in lower mantle Mg-perovskite, those of Fe^{3+} and Al^{3+}, can occur via one of 3 reactions:

$$M^{3+}{}_2O_3 = M^{3+}{}_m + M^{3+}{}_s + 3O_o \quad (1)$$

$$M^{3+}{}_2O_3 + 2Si_s + O_o = 2M^{3+}{}_s + \square_o + 2SiO_2 \quad (2)$$

$$M^{3+}{}_2O_3 + 3Mg_m = 2M^{3+}{}_m + \square_m + 3MgO, \quad (3)$$

Where the subscripts m, o and s represent the metal, oxygen, and silicon sites in perovskite, and $\square_o$ and $\square_m$ represent O and Mg vacancies, respectively.

Recent studies (Wood and Rubie 1996; Brodholt 2000; Lauterbach et al. 2000) suggested that Al plays a fundamental role in moderating the point defect chemistry of Mg-perovskite, being incorporated via reaction 1 (with either Fe^{3+} or Al^{3+} on the cation site) or reaction 2 (with oxygen vacancies) depending on the pressure, temperature, and chemical composition. Moreover, although several authors have reported that Al-bearing, Mg-perovskite is considerably more compressible than Al-free compositions, there are large discrepancies among the various studies, probably related to differences in the defect chemistry of the samples. Crystal-chemical studies of defective Mg-perovskite are, therefore, central to our understanding of the physical properties of lower-mantle Mg-perovskite.

Synthesis of large Mg-perovskite single crystals has been described previously (Ito and Weidner 1986), however, there are no reports of large Fe- or Al-bearing, high-quality, Mg-perovskite single crystals, or the attendant single-crystal studies. Flux-growth is a common technique for growing large single crystals of refractory salts and oxides at atmospheric pressure, and the principle is occasionally employed at high pressure to enhance reaction rates in solid-state equilibrium studies (e.g., Gasparik 1990). These studies often suffer from contamination of the phases of interest by the flux; however, the successful flux-growth of inclusion- and contamination-free olivine in the multi-anvil press was reported recently (Keppler et al. 2003).

Here, we present a flux-growth technique to produce large (up to 350 μm), high-quality, Mg-perovskite single crystals with compositions relevant to Earth's lower mantle. The newly available large Mg-perovskite crystals will make possible a wide range of new single-crystal experimental studies. The Mg-perovskite was grown in a molten NaCl flux at pressures and temperatures similar to normal synthesis conditions (24–25 GPa, 1900 °C, 2 h), with only a small amount of contamination by Na in the Mg-perovskite. This contamination might be avoided through use of an $MgCl_2$ flux. Recovered Mg-perovskite crystals are idiomorphic, with dominant pseudocube and less well developed octahedral morphologies, and strain- and inclusion-free. As a demonstration of the quality of the crystals produced by this method, a single-crystal structure refinement of Mg-perovskite (with composition $Mg_{1.00}Na_{0.01}Si_{0.99}O_{2.98}$) is presented.

* E-mail: d.dobson@ucl.ac.uk
† Present address: Geophysical Laboratory, Carnegie Institute of Washington, 5251 Broad Branch Road N.W., Washington D.C. 20015

EXPERIMENTAL METHODS

Equipment and methods

Mg-perovskite crystals were flux-grown in a 1000 ton, 6–8 type split-cylinder, multi-anvil-press installed at the Bayerisches Geoinstitute. Cr-doped MgO octahedra of 10 mm edge-length were compressed by Krupps tungsten carbide cubes with corners truncated to 4 mm edge length. A semiconducting $LaCrO_3$ furnace provided electrical heating, and the sample temperature was monitored via a W97Re3/W75Re25 thermocouple: no corrections for pressure were applied to the measured thermocouple emf. Starting glasses were prepared by fusing mixtures of SiO_2, MgO, Fe_2O_3, Al_2O_3, and Na_2CO_3 at 1650 °C and then reducing Fe-bearing compositions in H_2 at 1000 °C. Glass powders were packed in Re-foil capsules to half of the capsule length with the remaining capsule volume being filled with NaCl. The capsules were not welded shut; rather, the high experimental pressures were sufficient to seal overlapping layers of rhenium foil. Completed capsules were 2 mm long and 1.2 mm in diameter and were stored in a vacuum oven at ~200 °C. The high-pressure cell assembly has been described elsewhere (e.g., Dobson et al. 2002). High-pressure experiments were performed by room temperature compression to the desired load (equivalent to 24.5 GPa sample pressure) and subsequent heating. Experiments were quenched by cutting power to the furnace, which results in quench rates in excess of 500 °C/s, and subsequent slow decompression over ~15 hours.

Temperature-time path

Flux growth of large single crystals requires careful control of the temperature-time (*T-t*) path to ensure that the system remains in the growth dominated rather than nucleation dominated regime. The optimal *T-t* path used in the synthesis experiments reported here is cartooned in Figure 1. The essential points are:

(1) In order to reduce the level of $MgSiO_3$ superstauration in the NaCl flux, the glass was first transformed to Mg-perovskite below the NaCl melting temperature. Initial experiments suggested this was around 1850 °C at 25 GPa.

(2) The temperature was increased to several hundred decrees above the system solidus for several tens of minutes, after which the sample was cooled by ~50 °C and maintained at constant temperature for 30 minutes. The rapid cooling produces small Mg-perovskite seeds scattered throughout the flux.

(3) The temperature was then increased by 25 °C to dissolve the smaller seed crystals.

(4) A cyclical heating-cooling path was then followed, in which the temperature was slowly cooled (~2 °C/min) by 100 °C followed by rapid heating by 50 °C. This complex cooling path allows existing seed crystals to grow during cooling, while dissolving smaller new crystallites during the heating phase.

The *T-t* path described above results in a loosely intergrown aggregate of euhedral Mg-perovskite crystals around 100 μm across (Fig. 2a). A simple heating path consisting of transformation to Mg-perovskite at 1750 °C, followed by recrystallization at 1900 °C, results in large subhedral crystals growing from nucleation sites on the original Mg-perovskite surface. Although this procedure **{{AU: OK?}}** can produce larger crystals, 300 μm or more across, they tend to be strongly bonded to the Mg-perovskite substrate and more highly intergrown (Figs. 2b and 2c).

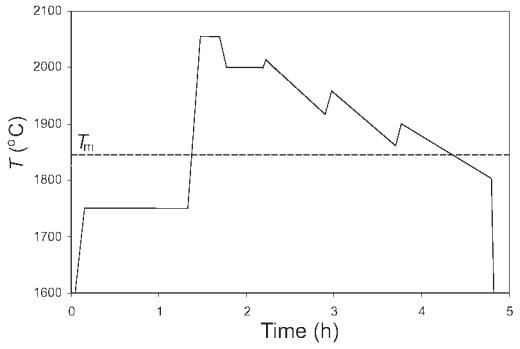

FIGURE 1. Schematic temperature-time path for perovskite growth experiments. T_m is the solidus for the $MgSiO_3$-NaCl system. Pressure was 24.5–25 GPa for all experiments.

RESULTS

Recovered samples were cleaned by dissolving the flux in distilled water and disaggregated by gently crushing under liquid-nitrogen. Handling Mg-perovskite under cryogenic temperatures can prevent the amorphization of this highly metastable phase under the stress of crushing.

Images of recovered flux-grown Mg-perovskite crystals are presented in Figure 2. The dominant pseudocube growth habit with minor octahedral modifications is in agreement with a recent prediction based on *ab initio* surface energy calculations (Alfredsson et al. 2004).

Composition

One portion of the run product from each experiment was mounted and coated with ~10 nm of carbon for chemical analysis using a JEOL 733 electron microprobe. Samples were not polished; analyses were performed on as-grown crystal facets oriented approximately perpendicular to the incident electron beam. A 2 mA, 15 kV beam with a spot size of about 1 μm was used for analysis. Electron probe totals ranged from 95 to 105 wt%, which is probably due to misorientations of analysed crystal facets relative to the electron beam and to amorphization of the analysed volume by the electron beam. The chemical compositions, presented in Table 1, have therefore been normalized to 100 wt%. All Mg-perovskite compositions produced by the current flux-growth method include a small contamination from Na (Cl was not detected). It is notable that the maximum Na content is attained in the Fe-bearing, Mg-perovskite composition—higher even than the Mg-perovskite with Na in the starting glass. This result suggests that Fe^{3+} on the Mg site not only aids incorporation of Al on the Si site but also aids incorporation of Na^+ cations on the Mg site. Such a supposition is supported by presence of small but significant cation excesses in the Na-bearing and Al-bearing compositions, but not in the Fe-bearing composition, as noted for Al-bearing compositions by previous workers (Ito et al. 1998; Andrault et al. 1998; McCammon et al. 1999). The low Al contents of the Mg-perovskites compared with starting glasses is due to the low synthesis pressure: Irifune et al. (1996) demonstrated that Al solubility in Mg-perovskite increases with

TABLE 1. Compositions of starting glasses and recovered perovskite crystals

	Perovskite		Fe-perovskite		Al-Perovskite	
	glass	perovskite	glass	perovskite	glass	perovskite
Na_2O	0.09	0.24 (02)	0.0	0.53 (03)	0.0	0.40 (02)
MgO	40.00	40.32 (80)	36.64	37.09 (70)	37.76	39.34 (04)
Al_2O3	0.0	–*	5.15	1.00 (04)	5.03	2.11 (04)
SiO_2	59.90	59.44 (70)	54.58	58.61 (40)	57.21	58.16 (05)
FeO†	0.0	–	3.63‡	2.77 (30)	0	-
Na		0.02		0.03		0.03
Mg		2.01		1.87		1.96
Al		0		0.04		0.08
Fe		0		0.08		0
Si		1.99		1.99		1.95
O		6		6		6
Cation§		4.02		4.01		4.02

Notes: Probe analyses of recovered perovskites normalized to 100%; see text for details.
* Not detected.
† Iron is assumed ferrous.
‡ Fe_2O_3 recalculated as FeO.
§ Based on 6 O atoms.

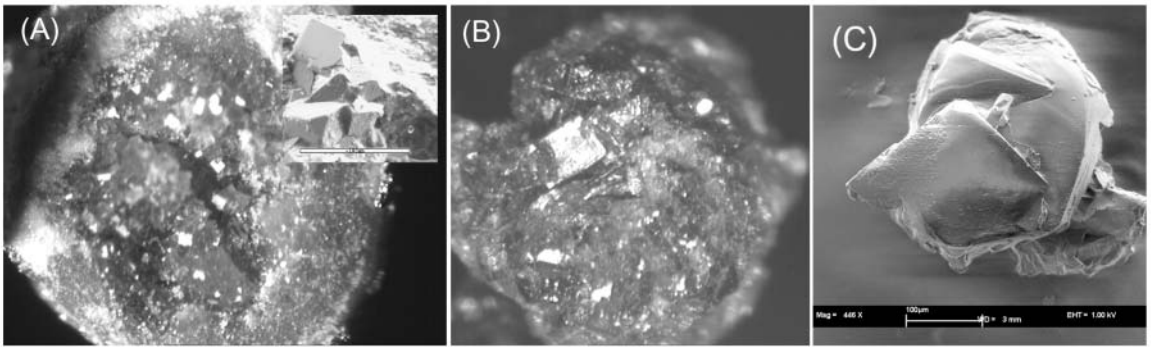

FIGURE 2. Flux-grown magnesium-silicate perovskites. (**A**) Al-bearing perovskite grown using the *T-t* path shown in Figure 1. Inset: Secondary electron image of substrate crystals showing dominant pseudo-cube with minor octahedral morphology. (**B**) Al- and Fe-bearing perovskite grown at 1900 °C. The field of view for figures A and B is approximately 1.2 mm. (**C**) Secondary electron image of "pure" $MgSiO_3$ perovskite grown at 1900 °C. Fluorite-type twinning is common in crystals from this experiment. Resorbtion features are probably due to small (±15 °C) temperature fluctuations during the experiment.

increasing pressure, reaching ~10 wt% at 27 GPa. There is no reason to suppose that this will not also be the case with NaCl-flux-grown Mg-perovskites. Excess Al was incorporated into majorite, one grain of which was identified by micro-raman spectroscopy. X-ray element mapping of a polished section of one Fe and Al-bearing Mg-perovskite crystal demonstrated that there is no chemical zonation in the flux-grown crystals (Fig. 3).

Single-crystal X-ray diffraction (XRD)

Single crystals of pure Mg-perovskite and $(Mg,Fe,Al)(Sl,Al)O_3$-perovskites measuring approximately $0.15 \times 0.15 \times 0.2$ mm and $0.25 \times 0.25 \times 0.35$ mm, respectively, were selected for XRD analysis based on their large sizes and clean optical extinction. The samples were centered on the Huber four-circle diffractometer at the Bayerisches Geoinstitut using an unfiltered Mo sealed-tube X-ray source. This instrument is optimized for determining cell parameters to high precision; the crystal is positioned about 45 cm from the X-ray source, 40 cm from the detector, and the X-ray beam is collimated by a 0.5 mm aperture near the source. Average peak widths (FWHM) were about 0.11 and 0.15 degrees-ω for the pure Mg- and the $(Mg,Fe,Al)(Si,Al)O_3$-perovskites, respectively. About thirty independent reflections with $10° \le 2\theta \le 35°$ were centered at eight equivalent positions following the procedure of King and Finger (1979). Unconstrained least-squares fitting to the peak positions (Ralph and Finger 1982) resulted in lattice angles $\alpha = 90.004(4)°$, $\beta = 90.004(4)°$, and $\gamma = 89.993(4)°$ for the pure Mg-perovskite crystal, and $\alpha = 90.004(5)°$, $\beta = 89.999(4)°$, and $\gamma = 90.001(4)°$ for the $(Mg,Fe,Al)(Si,Al)O_3$-perovskite. The orthorhombic cell

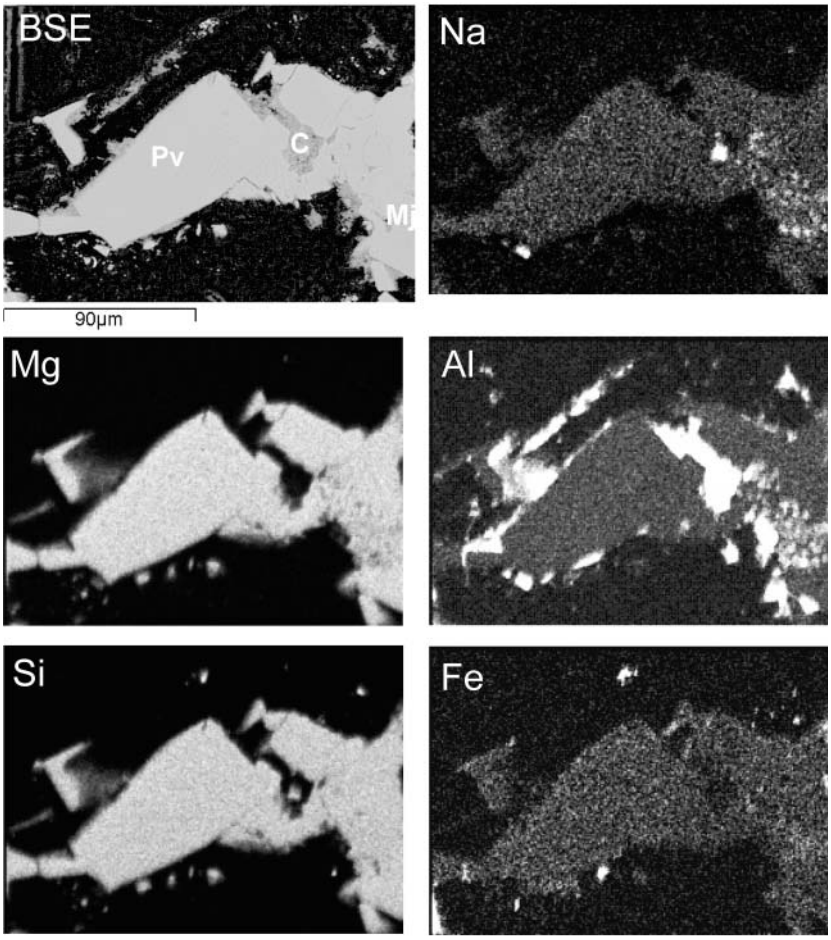

FIGURE 3. X-ray element map of polished section of iron and aluminium bearing perovskite crystals (from the sample displayed in Figure 2b). The phases labelled on the back-scattered electron image are: Pv-perovskite, Mj-majorite, and C-corundum. The corundum is contamination from polishing and the dark background material is cyanoacrylate based resin. The element maps are displayed in linear greyscale with full scales of: Na$K\alpha$ 0-15 counts, Mg$K\alpha$ 0–130 counts, Al$K\alpha$ 0–60 counts, Si$K\alpha$ 0–150 counts, and Fe$K\alpha_1$ 0–20 counts. There is no detectable zonation in the perovskite crystals.

for both compositions is reported in Table 2. We observed a relatively small (0.3%) volume increase for the Fe- (0.08 per formula) and Al- (0.04 per formula) bearing perovskite compared to the pure Mg- perovskite. Calculated densities are 4.104(1) and 4.138(1) g/cm^3 for the pure Mg- and (Mg,Fe,Al)(Al,Si)O_3-perovskite, respectively.

The crystal of pure Mg-perovskite was mounted on an Enraf Nonius CAD4 X-ray diffractometer for intensity data collection. A four-times redundant hemisphere of reciprocal space was visited with $h \pm 7°$, $k \pm 7°$, and $l + 11°$, resulting in 1511 total reflections with $5° \leq 2\theta \leq 70°$ and an average $I/\sigma(I) = 20.2$. Symmetry equivalent reflections were merged ($R_{int} = 0.06$) and corrected for Lorentz and polarization effects, resulting in 372 unique observations. The data were not corrected for absorption because of the very low Mo$K\alpha$ X-ray absorption coefficient, $\mu = 1.41$/mm. The structure was refined on F^2 in space group *Pbnm* using the *WinGX* package of SHELX-97 (Farrugia 1999; Sheldrick 1997) with initial atom positions from Horiuchi et al. (1987). After refinement of anisotropic displacement parameters, the final model *R*-factor (on F^2) is 0.064 using all the data, or $R(F) = 0.024$ for $F_o > 4\sigma(F_o)$. The goodness of fit for the refinement is 1.044. Atom position and displacement parameters are given in Tables 3 and 4. Bond distances and polyhedral bond lengths and angles are presented in Table 5.

Table 2. Cell parameters of flux-grown pure-$MgSiO_3$ and (Mg,Fe,Al)(Al,Si) perovskites

	pure-$MgSiO_3$	$(Mg_{1.87}Fe_{0.08}Al_{0.04})SiO_3$
a	4.7780(2) Å	4.7824(3) Å
b	4.9298(3)	4.9358(4)
c	6.8990(3)	6.9095(3)
Vol	162.502(14) Å^3	163.100(17) Å^3
ρ_{calc}	4.104(1) g/cm^3	4.138(1) g/cm^3
eight-position centering		
average FWHM (ω)	0.113°	0.148°

Table 3. Structure of $MgSiO_3$-perovskite in *Pbnm*

	x/a	*y/b*	*z/c*
Mg	0.51378(12)	0.55588(14)	¼
Si	½	0	½
O1	0.10189(26)	0.46645(25)	¼
O2	0.19626(18)	0.20133(17)	0.55258(12)

Table 4. Anisotropic displacement parameters (×100) for $MgSiO_3$-perovskite in *Pbnm*

	U_{11}	U_{22}	U_{33}	U_{12}	U_{13}	U_{23}	U_{eq}
Mg	0.77(3)	0.64(3)	1.06(3)	0.05(2)	0	0	0.83(2)
Si	0.55(2)	0.50(2)	0.69(2)	–0.03(1)	0.02(1)	–0.01(1)	0.58(1)
O1	0.73(5)	0.71(4)	0.75(4)	–0.01(4)	0	0	0.73(2)
O2	0.69(3)	0.62(3)	0.95(3)	0.09(3)	0.09(2)	0.06(3)	0.75(2)

Table 5. Polyhedral bond lengths for flux-grown $MgSiO_3$-perovskite

Central atom		*R*(*X*-O) Å
Si	O1 (×2)	1.7829(8)
	O2 (×2)	1.7952(8)
	O2 (×2)	1.7998(4)
	average	1.793
R(Mg-O)<2.8 Å	O1	2.017(1)
	O2 (×2)	2.055(1)
	O1	2.098(1)
	O2 (×2)	2.282(1)
	O2 (×2)	2.425(1)
	average	2.205
R(Mg-O) > 2.8 Å		
	O1	2.844(1)
	O1	2.957(1)
	O2 (×2)	3.117(1)

Disscusion

We refined the structure of our flux-grown Mg-perovskite to demonstrate the quality of the samples and because it is one of the largest single crystals ever reported. The main aspects of the structure (such as the space group and polyhedral distortions and rotations) are consistent with previous diffraction studies (Ito and Matsui 1978; Yagi et al. 1978; Horiuchi et al. 1987; Kudoh et al. 1987; Ross and Hazen 1990). Mg-perovskite is related to real perovskite ($CaTiO_3$) by substitution of Mg for Ca and Si for Ti. In this respect, Mg-perovskite is an octahedral framework silicate (Ross 2001). The MgO_{12} cuboctahedra share every edge with either another MgO_{12} polyhedron or a silicate octahedron, which are completely corner sharing with each other. Silicon lies on the inversion centre of symmetry (in *Pbnm*) forming an undistorted silicate octahedron. The silicate octahedra share triangular faces with the cuboctahedra, forming an irregular MgO_{12} polyhedron, with eight *R*(Mg-O) distances less than 2.8 Å and four with 2.8 Å<*R*(Mg-O)<3.12 Å. Polyhedral bond lengths for flux-grown Mg-perovskite are listed in Table 5.

To test for significant occupancy of the Mg site by Na, or Mg-Si disorder in the octahedral site as in γ-Mg_2SiO_4 (ringwoodite), once the structure model was complete we allowed the site-occupancy factors (s.o.f. = multiplicity of site / multiplicity of general position) to refine separately. At the Mg site, the s.o.f. is reduced insignificantly to 0.496(2) or 99.2%, equivalent to 11.90(5) electrons. At the octahedral site, the s.o.f. is insignificantly above full with s.o.f. = 0.502(3) or 14.06(8) electrons. Any Na in the structure is expected to occupy the Mg site due to the similarity in charge and ionic radii, as in the sodium tungstate (Na_xWO_3) perovskites.

The high-pressure, flux-growth technique presented here yields large, high quality single crystals of perovskite-type $(Mg,Fe,Al,Na)(Si,Al)O_3$ that can be readily separated and studied. Electron probe analysis shows that there is only minor incorporation (<1 at%) of Na from the flux into the perovskite structure, and that this impurity can be enhanced by paired heterovalent substitutions. Chlorine was not detected in any recovered perovskite samples. We suggest, therefore, that $MgCl_2$ might be used as a flux for Mg-perovskite growth with potentially zero undesirable contamination of the resultant crystals. Synthesis of large $(Mg,Fe,Al)(Si,Al)O_3$-perovskite has especially important applications to mineral physics and the Earth sciences because this phase should dominate in Earth's lower mantle, making it the most abundant silicate in the planet. The unprecedented large size of the crystals (>250 μm) makes possible a whole suite of single-crystal experimental techniques not previously possible for Mg-perovskite due to the normally small (<50 μm) grain sizes of synthetic perovskite.

Acknowledgments

Both authors were supported by Alexander von Humboldt Fellowships and DPD is grateful in addition to the Royal Society for his University Research Fellowship. We wish to thank T. Boffa-Ballaran, F. Heidelbach, and A. Beard for the use of their instruments. This paper was improved by the helpful suggestions of B. Hazen and one anonymous reviewer.

REFERENCES CITED

Alfredsson, M., Dobson, D.P., Oganov, A.R., Catlow, C.R.A., Brodholt, J.P., Parker, S.C., and Price, G.D. (2004) Crystal morphology and surface structures of the orthorhombic $MgSiO_3$ perovskite. Physics and the Chemistry of Minerals, in press.

Andrault, D., Neuville, D.R., Flamk, A.M., and Wang, Y. (1998) Cation sites in Al-rich $MgSiO_3$ perovskites. American Mineralogist, 83, 1045–1053.

Brodholt, J.P. (2000) Pressure-induced changes in the compression mechanism of aluminous perovskite in the Earth's mantle. Nature, 407, 620–622.

Dobson, D.P., Vocadlo, L., and Wood, I.G. (2002) A new high-pressure phase of FeSi. American Mineralogist, 87, 784–787.

Dziewonski, A.M. and Anderson, D.L. (1981) Preliminary reference Earth model. Physics of Earth and Planetary Interiors, 25, 297–356.

Farrugia, L.J. (1999) *WinGX* suite for small-molecule single-crystal crystallography. Journal of Applied Crystallography, 32, 837–838.

Gasparik, T. (1990), A thermodynamic model for the enstatite-diopside join. American Mineralogist, 75**,** 1080–1091.

Horiuchi, H., Ito, E., and Weidner, D.J. (1987) Perovskite-type $MgSiO_3$: single-crystal X-ray diffraction study. American Mineralogist, 72, 357–360.

Irifune, T., Tomomi, K., and Jun-ichi, A. (1996) An experimental study of the garnet-perovskite transformation in the system MgO_3-$Mg_3Al_2Si_3O_{12}$. Physics of Earth and Planetary Interiors, 96, 147–157.

Ito, E. and Matsui, Y. (1978) Synthesis and crystal-chemical characterization of $MgSiO_3$ perovskite. Earth and Planetary Science Letters, 38, 443–450.

Ito, E. and Weidner, D.J. (1986) Crystal-growth of $MgSiO_3$ perovskite. Geophysical Research Letters, 13, 464–466.

Ito, E., Kubo, A., Katsura, M., Akaogi, M., and Fujita, T. (1998) High-pressure transformation of pyrope ($Mg_3Al_2Si_3O_{12}$) in a sintered diamond cubic anvil assembly. Geophysical Research Letters, 25, 821–824.

Keppler, H., Wiedenbeck, M., and Shcheka, S.S. (2003) Carbon solubility in olivine and the mode of carbon storage in the Earth's mantle. Nature, 424, 414–416.

King, H. and Finger, L.W. (1979) Diffracted beam crystal centering and its application to high-pressure crystallography. Journal of Applied Crystallography, 12, 374–378.

Kudoh, Y., Ito, E., and Takeda, H. (1987) Effect of pressure on the crystal structure of perovskite-type $MgSiO_3$. Physics and Chemistry of Minerals, 14, 350–354.

Lauterbach, S., McCammon, C.A., van Aken, P., Langebhorst, F., Seifert, F. (2000) Mössbauer and ELNES spectroscopy of $(Mg,Fe)(Si,Al)O_3$ perovskite: a highly oxidised component of the lower mantle. Contributions to Mineralogy Petrology, 138, 17–26.

McCammon, C., Langenhorst, F., and Seifert, F. (1999) How well do we know the properties of lower mantle perovskites? Eos, 80, F742.

Ralph, R.L. and Finger, L.W. (1982) A computer program for refinement of crystal orientation matrix and lattice constants from diffractometer data with lattice symmetry constraints. Journal of Applied Crystallography, 15, 537–539.

Ross, N.L. (2001) Framework structures. In R.M. Hazen and R.T. Downs, Eds., High-temperature and high-pressure crystal chemistry, 41, 257–287. Reviews in Mineralogy and Geochemistry, Washington, D.C.

Ross, N.L. and Hazen, R.M. (1990) High pressure crystal chemistry of $MgSiO_3$ perovskite. Physics and Chemistry of Minerals, 17, 228–237.

Sheldrick, G. (1997) SHELXL-97—A program for crystal structure refinement. University of Göttingen, Germany, Release 97–2.

Wood, B.J. and Rubie, D.C. (1996) The effect of alumina on phase transformations at the 660-kilometer discontinuity from Fe-Mg partitioning experiments. Science, 273, 1522–1524.

Xu, Y. and McCammon, C. (2002) Evidence for ionic conductivity in lower mantle $(Mg,Fe)(Si,Al)O_3$ perovskite. Journal of Geophysical Research, 107, article no. 2251.

Xu, Y., McCammon, C., and Poe, B.T. (1998) The effect of alumina on the electrical conductivity of silicate perovskite. Science, 282, 922–924.

Yagi, T., Mao, H.K., and Bell, P.M. (1978) Structure and crystal chemistry of perovskite-type $MgSiO_3$. Physics and Chemistry of Minerals, 3, 97–110.

Zhang, J. and Weidner, D.J. (1999) Thermal equation of state of aluminium-enriched silicate perovskite. Science, 284, 782–784.

MANUSCRIPT RECEIVED SEPTEMBER 29, 2003
MANUSCRIPT ACCEPTED FEBRUARY 2, 2004
MANUSCRIPT HANDLED BY ALISON PAWLEY